

Supporting Information for “Rapid phytoplankton response to wind forcing influences productivity in upwelling bays”

E. Broullón¹, P. J. S. Franks², B. Fernández Castro³, M. Gilcoto⁴,
A. Fuentes-Lema¹, M. Pérez-Lorenzo¹, E. Fernández¹, and B.
Mouriño-Carblido¹

¹Centro de Investigación Mariña da Universidade de Vigo
(CIM-UVigo), Vigo, Spain

²Scripps Institution of Oceanography, University of California San
Diego, La Jolla, CA, USA

³Ocean and Earth Science, National Oceanography Centre,
University of Southampton, Southampton, UK

⁴Departamento de Oceanografía, Instituto de Investigacións
Mariñas (IIM-CSIC), Vigo, Spain

Contents of this file

1. Text S1
2. Figures S1 to S4

1 Text S1

1.1 Dynamical equations for the barotropic response of the ría

The analyses included in this supplementary material are based on the previous observational study carried out by Gilcoto *et al.* (2017), which showed a rapid response of the ocean-bay exchange flow to wind forcing within the Galician Rías. Here, we intend to complete this observational analysis with a mechanistic approach showing that these rapid dynamics in the rías could be explained by the barotropic response to wind forcing, and their associated time scales.

Let's take the ría as a rectangular channel extending in the x direction (the y direction is assumed to be irrelevant, as we neglect rotation) with a length L and a sea-surface height h at equilibrium, and study the barotropic response to an along-channel wind stress (τ_w). At the west end of the ría, the height is fixed (we assume that the volume of the adjacent ocean is infinite), and at the inner eastern end the surface position can vary. We define the surface height anomaly with respect to the equilibrium as η (Figure S2).

The response is determined by the continuity equation and the momentum equation in the x axis. We reduce the problem to two dimensions by resolving the eastward velocity, $u(z, t)$, of the ría at its mouth ($x = 0$). We take the origin at the bottom ($z = 0$). The continuity equation:

$$\frac{\partial u}{\partial x} + \frac{\partial v}{\partial y} + \frac{\partial w}{\partial z} = 0 \quad (1)$$

is reduced to two dimensions and written in an integral form:

$$\int_0^h \frac{\partial u}{\partial x} dz + \frac{\partial \bar{\eta}}{\partial t} = h \frac{\partial \bar{u}}{\partial x} + \frac{\partial \bar{\eta}}{\partial t} = 0 \quad (2)$$

where $\bar{\eta}$ is the mean height within the ría, which corresponds to half of the height in the eastern-most point, $\bar{\eta} = \eta/2$. Because the eastward velocity is zero at the solid wall ($x = L$):

$$\frac{\partial \bar{u}}{\partial x} = \frac{\bar{u}(x = L) - \bar{u}(x = 0)}{L} = -\frac{\bar{u}(x = 0)}{L} \equiv -\frac{\bar{u}}{L} \quad (3)$$

So then we have as continuity equation:

$$\boxed{\frac{\partial \eta}{\partial t} = 2h \frac{\bar{u}}{L}} \quad (4)$$

On the other hand, the momentum equation in the x direction is:

$$\frac{Du}{Dt} = fv - \frac{1}{\rho} \left(\frac{\partial p}{\partial x} + \frac{\partial \tau_x}{\partial z} \right) \quad (5)$$

28 We neglect the non linear terms ($\frac{Du}{Dt} \approx \frac{\partial u}{\partial t}$), and also Coriolis acceleration
 29 ($fv \approx 0$), and we follow a hydrostatic approximation ($p = g\rho(z + \eta)$). Because
 30 at $x = 0$, $\eta = 0$, for every z :

$$\frac{\partial p}{\partial x} = \frac{p(x=L) - p(x=0)}{L} = \frac{g\rho\eta}{L} \quad (6)$$

31 Where we assumed that p increases linearly with x . We model the shear stresses
 32 with a turbulent viscosity (κ):

$$\tau_x(z, t) = -\rho\kappa \frac{\partial u}{\partial z}(z, t) \quad (7)$$

33 With all this, the momentum equation is reduced to:

$$\boxed{\frac{\partial u}{\partial t} = -\frac{g\eta}{L} + \kappa \frac{\partial^2 u}{\partial z^2}} \quad (8)$$

34 with boundary conditions:

$$u(z=0) = 0 \quad (9)$$

35 and

$$\rho\kappa \frac{\partial u}{\partial z}(z=h) = \tau_w \quad (10)$$

36 where we calculated

$$\tau_w = \rho_{air} C_D W^2 \quad (11)$$

37 To illustrate this non-rotational barotropic response of the ría to an along-
 38 channel wind pulse we performed a simulation using equations 4, and 8 to
 39 11, by taking $h = 40$ m, $L = 30$ km, $g = 9.81$ m s⁻², $\rho_a = 1.2$ kg m⁻³,
 40 $\rho = 1000$ kg m⁻³, $C_D = 10^{-3}$ and $\kappa = 5 \times 10^{-4}$ m² s⁻¹. The wind was set
 41 to $W = -10$ m s⁻¹ (offshore) between days 2 and 5 of the simulation. A 30
 42 day spin-up was used to allow the system to equilibrate and damp oscillations.
 43 Figure S3 shows the result of the simulation. As soon as the wind starts blowing,
 44 the water level inside the ría drops by ~ 20 cm and starts oscillating at relatively
 45 high frequency (< 1 h). At the same time a bidirectional flow, with outflowing
 46 surface layer and inflowing bottom layer starts to develop immediately, first
 47 with strong linear acceleration, and equilibrates slowly (due to the action of
 48 viscosity) over the duration of the wind pulse (3 days, a typical value for the
 49 system). However, full equilibrium seems not to be reached.

50 There are two inherent time-scales to this response. First, the barotropic
 51 along-ría time-scale which determines the propagation of the pressure pertur-
 52 bation signal along the channel, and an equilibration time-scale which depends
 53 on the damping effect of viscosity. The barotropic time scale can be deter-
 54 mined by neglecting the viscous term in Eq. 8 (second term on the right hand
 55 side), and by derivating and substituting with Eq. 4, taking into account that
 56 for a barotropic response without friction or wind forcing the velocity profile is
 57 uniform, $u(z) = \bar{u}$:

$$\frac{\partial^2 u}{\partial t^2} = -\frac{g}{L} \frac{\partial \eta}{\partial t} \Rightarrow \frac{\partial^2 u}{\partial t^2} = -\frac{2hg}{L^2} u \quad (12)$$

58 This is the equation for an harmonic oscillation with frequency $\omega = (\frac{2hg}{L^2})^{1/2}$.
 59 Hence, the barotropic period is:

$$T_{bt} = 2\pi\omega^{-1} \approx 1.90 \text{ h} \quad (13)$$

60 So the barotropic response of the ría starts to develop in less than a couple
 61 of hours. This is also the frequency of the oscillations observed in the water
 62 level. However, the acceleration time-scale (and the equilibrium exchange ve-
 63 locities) is dictated by the equilibrium between the pressure gradient and the
 64 frictional response. The equilibrium solution could be found analytically by
 65 taking $\frac{\partial u}{\partial t}, \frac{\partial \eta}{\partial t} = 0$ in Eq. 4 and 8. Because we are interested in the dynamic
 66 response (equilibration time), we performed instead three simulations with dif-
 67 ferent values of κ and for a wind pulse extending between days 2 and 10 of the
 68 simulation, in order to allow some extra time for equilibration (Figure S4). The
 69 different time-scales correspond to the response to the different viscosity values,
 70 instead to the wind intensity, since this takes a common value for the three
 71 cases. This figure shows that the equilibrium exchange velocities are larger for
 72 weaker viscosities. Viscosity values of $5 - 10 \times 10^{-4} \text{ m}^2 \text{ s}^{-1}$ produced realis-
 73 tic equilibrium exchange velocities (10-20 cm s^{-1}) (Barton *et al.*, 2015), but
 74 those were unrealistically high for a weaker viscosity of $\kappa = 0.1 \times 10^{-4} \text{ m}^2 \text{ s}^{-1}$.
 75 This figure also illustrates the linear response of the ría until the viscosity ef-
 76 fects become important for all viscosity values. Until a time scale t for which
 77 $u = u_{max}/2$, the response is almost linear. This time scale was about half a day
 78 (smaller than the local inertial period of 0.75 days) for $\kappa = 1 \times 10^{-4} \text{ m}^2 \text{ s}^{-1}$, and
 79 about 1 day for $\kappa = 5 \times 10^{-4} \text{ m}^2 \text{ s}^{-1}$. In all the three cases, the bidirectional
 80 circulation is set-up almost immediately, while a rotational response would take
 81 one inertial period or more, such that the along-shore circulation equilibrates
 82 with the Coriolis force.

83 1.2 Methods

84 Chlorophyll samples collected during the REMEDIOS-TLP cruise as well
 85 as other samples collected during the seasonal samplings of the REMEDIOS
 86 project (March 2017 to May 2018) were used to calibrate the MSS90 fluorescence
 87 sensor ($n = 65$). The fitted calibration curve was:

$$\text{chlorophyll } a = 1.460 \times \text{fluorescence} - 0.248, (R^2 = 0.901) \quad (14)$$

88 To calibrate the fluorescence sensor of the SBE911, a set of chlorophyll sam-
 89 ples collected during the cruise at different stations throughout the study area
 90 was used ($n=71$):

$$\text{chlorophyll } a = 0.270 \times \text{fluorescence} - 0.051, (R^2 = 0.855) \quad (15)$$

91 Primary production rates were determined by running incubations with the
 92 radioisotope ^{14}C as described in Cermeño *et al.* (2016). Briefly, four 72 ml acid-
 93 washed polystyrene bottles (three light and one dark bottle) were filled with sea-
 94 water from each depth. Each bottle was inoculated with $\sim 5\text{-}9 \mu\text{Ci}$ of $\text{NaH}^{14}\text{CO}_3$

95 and then incubated for 2 h starting at noon. Three incubators equipped with
96 a set of blue and neutral density plastic filters were used to simulate irradiance
97 conditions at the original sampling depths (surface, deepest and intermediate
98 depths). Temperature conditions during the incubation period were kept simi-
99 lar to those observed at the different sampling depths ($\pm 3^{\circ}\text{C}$) by employing a
100 closed refrigerated water system. Immediately after incubation, samples were
101 filtered through $0.2\ \mu\text{m}$ polycarbonate filters under low-vacuum pressure. Non-
102 assimilated radioactive inorganic carbon retained in the filters was removed by
103 exposing them to concentrated HCl fumes overnight. Radioactivity signal on
104 each sample was determined on a 1414 Wallac Scintillation counter, which used
105 an internal standard for quenching correction.

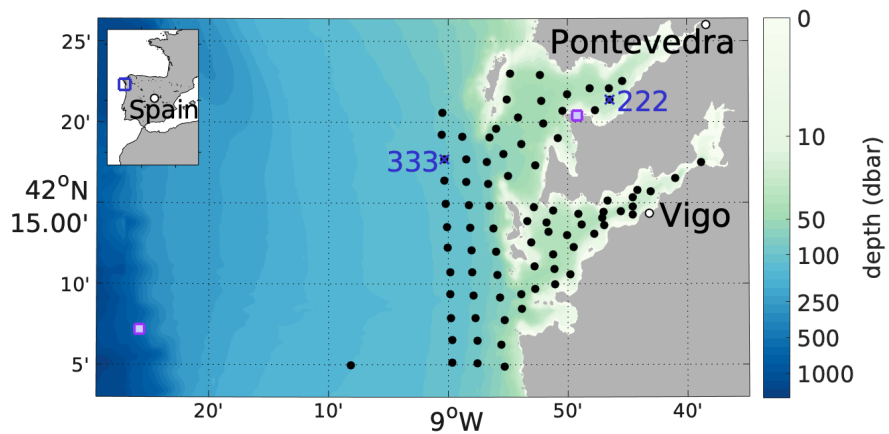


Figure S1: Bathymetry map of the two southernmost Galician Rías Baixas: Ría de Pontevedra and Ría de Vigo, and the adjacent shelf. The sampling area is located at the northern end of the Canary Current-Iberian Upwelling System where the regional circulation is affected by cycles of wind-driven upwelling and downwelling (Fraga 1981). The mean water depth in the sampling domain ranged from 15 to 60 m between the inner and outer parts of the bays, dropping sharply at their mouth to 115 m deep at the westernmost sampling points over the shelf break. Black dots indicate the sampling stations during REMEDIOS-TLP cruise. The blue crosses indicate the intensive sampling station, 222, and the shelf control station, 333. Purple squares indicate the shelf and Ría stations where wind data were measured. Bathymetry data from GEBCO Compilation Group 2020 (doi:10.5285/a29c5465-b138-234d-e053-6c86abc040b9).

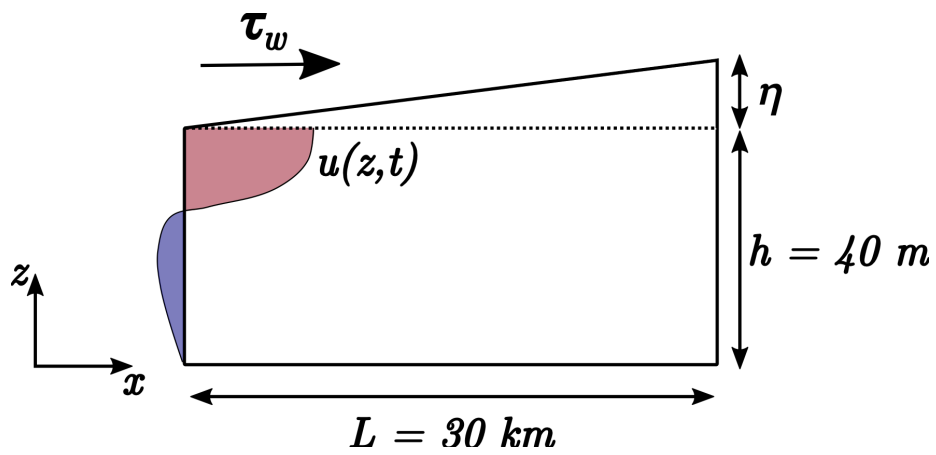


Figure S2: Schematic of the dynamical balance of barotropic response of the ría to an along-channel wind stress (τ_w).

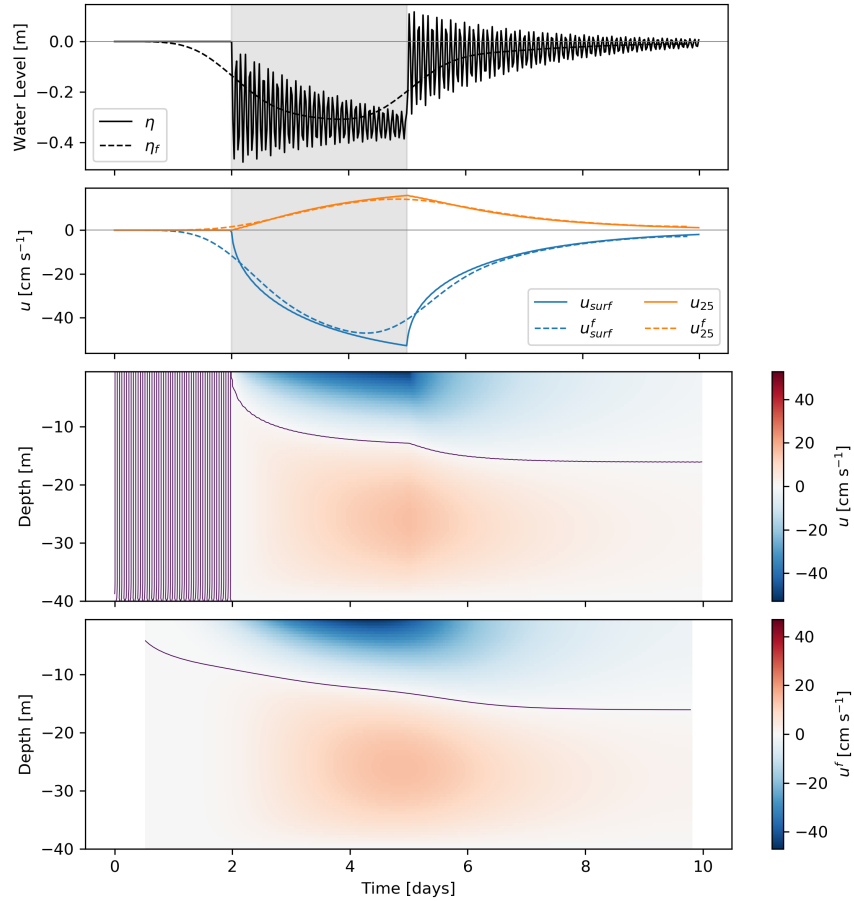


Figure S3: Simulation of the ría response to a down-channel wind pulse of $W = 10 \text{ m s}^{-1}$ during days 2-5 of the simulation using the barotropic model. Water level at the inner-most point (η) and eastward velocities (u) are shown. The f index indicates quantities filtered with a Godin 24/25/24 filter. In the second panel, the velocity at the surface layer ($z = 0.5 \text{ m}$) and at 25 m depth are displayed. In this simulation, the turbulent viscosity is set to $\kappa = 5 \times 10^{-4} \text{ m}^2 \text{ s}^{-1}$. Purple lines indicate zero values. Oscillations during days 0-2 are regular barotropic oscillations of the system, prior to the application of the forcing.

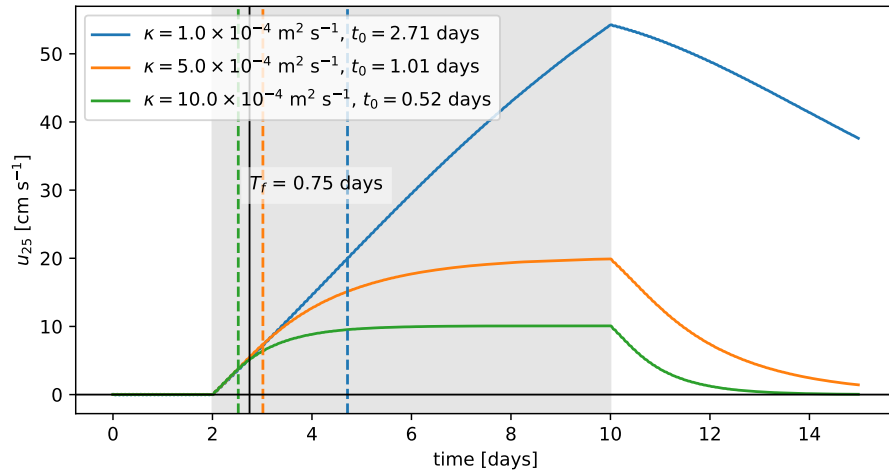


Figure S4: Along-channel velocities at 25 m depth for simulations of the barotropic non-rotational response of the ría to a wind pulse $W = -10 \text{ m s}^{-1}$ between days 2 and 10 of the simulation, with different values of the turbulent viscosity coefficient (κ). The response time (t_0) is the time required for u to reach $1/e$ of its maximum value. The inertial period T_f is shown for comparison.